ISSN 1070-3284, Russian Journal of Coordination Chemistry, 2013, Vol. 39, No. 7, pp. 524–528. © Pleiades Publishing, Ltd., 2013.

A New Layered Lead(II) MOF with Helical Chain Motif: Synthesis, Crystal Structure, and Fluorescence[1]

X. G. Wang, E. C. Wang, and E. C. Yang*

College of Chemistry, Tianjin Key Laboratory of Structure and Performance for Functional Molecules, Tianjin Normal University, Tianjin, 300387 P.R. China

**e-mail: encui_yang@yahoo.com.cn*

Received November 25, 2011

Abstract—A novel layered MOF, $\{[Pb_2(H_2Bic)(HBic)Cl_3] \cdot 2H_2O\}_n$ (**I**), was hydrothermally obtained by the reaction of $PbCl_2$ with 1-*H*-benzimidazole-5-carboxylic acid (H_2Bic) and fully characterized by single-crystal X-ray diffraction, elemental analysis, FT-IR, TG–DTA, and luminescent spectra. Structural analysis suggests that complex **I** is a 2D layer assembled from helical Pb(II)-$HBic^-$ chains and bridging chloride linkers, which is H-bonded together into a 3D supramolecular network. Additionally, **I** in the solid-state exhibits a favorable fluorescent emission at room temperature due to the intraligand charge transfer, suggesting its potential application as fluorescence materials.

DOI: 10.1134/S1070328413060110

INTRODUCTION

Metal-organic frameworks (MOFs) constructed from inorganic metal ions and various organic connectors have always received intense interest due to their fascinating and versatile structures [1], intriguing topologies [2], and promising chemical and/or physical properties in magnetism [3], luminescence [4], catalysis [5], and gas sorption [6]. It is well known that both the variable coordination polyhedra of the inorganic source and the tunable coordination modes of the function ligands play important roles on the framework connectivity and functionalized properties of the resulting MOFs. More interestingly, the overall framework of the target MOFs can also be greatly influenced by some external factors, such as template/guest molecules [7], pH value [8], preparation method [9], reaction temperature [10], and so on. Therefore, the self-assembly of the selected ligands with metal ions under different controllable conditions can be hopefully expected to produce surprising complexes with unpredictable structures and performances.

Possessing two imidazole N and two carboxylate O donors, 1-*H*-benzimidazole-5-carboxylic acid (H_2Bic) can selectively coordinate to metal ion by different bridging coordination modes (terminally monodentate-, chelating-/bridging-bidentate, and bridging-polydentate modes) and thus has behaved as a versatile linker to construct novel MOFs with abundant hydrogen bonds and π–π stacking interactions [11–16]. In particular, the changeable proton site between the carboxylic group and the imidazole ring and the deprotonation extent of the carboxylic group in H_2Bic ligand can be careful manipulated by careful control the pH value of the reaction mixture, which can make the H_2Bic-based metal complexes more challenge and more attractive. Additionally, the relatively large π-conjugated system by benzimidazole ring might contribute essentially to the desirable fluorescence property resulting from the possibly intraligand or ligand-to-metal charge transfer [13, 15]. However, to the best of our knowledge, only several Ni(II)-, as well as Cd(II)-, and Co(II)-based complexes with the deprotonated $HBic^-$ ligand [11–16] have been obtained up to date either by careful control of the pH value of the medium or by addition of the appropriate template molecules. On the other hand, inorganic Pb^{2+} ion with large ion radius, versatile coordination polyhedra, and possible occurrence of a stereochemically active lone pair of electrons has already is proved to be a favorable block to generate coordination polymers or polynuclear complexes [17]. Herein, to further investigate the H_2Bic-based functional molecular materials [11–16], synthesis and crystal structure of a new 2D layered Pb(II)-containing MOF named $\{[Pb_2(H_2Bic)(HBic)Cl_3] \cdot 2H_2O\}_n$ (I) with helical chain motif is reported, which with relatively higher thermal stability shows a strong luminescence at room temperature originating from the intraligand charge transfer.

EXPERIMENTAL

Reagents and instruments. 1-*H*-benzimidazole-5-carboxylic acid was purchased from Acros and other analytical-grade starting materials were obtained commercially and used as received without further purification. Doubly deionized water was employed for

[1] The article is published in the original.

the conventional synthesis. IR spectra were collected in a range of 4000–400 cm^{-1} region on a Nicolet IR-200 spectrometer as KBr pellets. Elemental analyses for C and H were determined on a PerkinElmer 2400C elemental analyzer. Thermogravimetric (TG) analysis was carried out on a Shimadzu simultaneous DTG-60A thermal analysis instrument with a heating rate of 10°C min^{-1} from room temperature to 800°C under a nitrogen atmosphere (flow rate 10 mL min^{-1}). Fluorescence spectra of the polycrystalline powder samples were performed on a Cary Eclipse fluorescence spectrophotometer (Varian) equipped with a xenon lamp and quartz carrier at room temperature.

Synthesis of I. $PbCl_2$ (27.8 mg, 0.1 mmol) and H_2Bic (16.2 mg, 0.1 mmol) were dissolved in doubly deionized water (10.0 mL). And the initial pH value of the mixture was adjusted to ~5 by triethylamine. The mixture was then transferred into a parr Teflon-lined stainless steel vessel (23.0 mL) and heated to 105°C for 24 h under autogenous pressure. After the mixture was cooled to room temperature at a rate of 1.1°C h^{-1}, colorless block-shaped crystals suitable for X-ray analysis were obtained directly, washed with water and ethanol, and dried in air. The yield was 45% based on $PbCl_2$.

For $C_{16}H_{15}Cl_3N_4O_6Pb_2$

anal. calcd., %:	C, 21.84;	H, 1.72;	N, 6.37.
Found, %:	C, 21.82;	H, 1.73;	N, 6.39.

IR (ν, cm^{-1}): 3482 ν_b(O–H), 1635 ν(C=N), 1537 $\nu_{as}(COO^-)$, 1511 $\nu_{as}(COO^-)$, 1406 $\nu_{as}(COO^-)$, 1408 $\nu_s(COO^-)$, 1377 $\nu_s(COO^-)$.

X-ray diffraction analysis. Structure measurement of **I** was performed on a computer controlled Bruker APEX-II CCD diffractometer equipped with graphite-monochromated MoK_α radiation with radiation wavelength of 0.71073 Å by using a ω–φ scan technique at 296(2) K. The program SAINT [18] was used for integration of the diffraction profiles. Semi-empirical absorption corrections were applied using SADABS [19] program. The structures were solved by direct methods and refined with the full-matrix least-squares technique using the SHELXS-97 and SHELXL-97 programs [20]. Anisotropic thermal parameters were assigned to all non-hydrogen atoms. The organic hydrogen atoms were generated geometrically. The starting positions of H attached to oxygen atom were located in difference Fourier syntheses and then fixed geometrically as riding atoms. The crystallographic data, selected bond lengths, and angles are listed in Tables 1, 2. Hydrogen-bonding parameters are given in Table 3. Supplementary material has been deposited with the Cambridge Crystallographic Data Centre (no. 822276; deposit@ccdc.cam.ac.uk or http://www.ccdc.cam.ac.uk).

Table 1. Crystallographic data and experimental details for complex **I**

Parameter	Value
Formula weight	880.05
Crystal size, mm	0.15 × 0.12 × 0.10
Crystal system	Monoclinic
Space group	*C*2/*c*
a, Å	24.5215(9)
b, Å	7.1211(2)
c, Å	25.2072(9)
β, deg	104.0750(10)
V, $Å^3$	4269.5(2)
Z	8
ρ_{calcd}, g/cm^3	2.738
μ_{Mo}, mm^{-1}	16.171
F(000)	3216
θ Range, deg	2.66–25.01
Range of reflection indices	$-28 \le h \le 28$, $-7 \le k \le 8$, $-29 \le l \le 19$
Reflections collected/unique	10289/3712
R_{int}	0.0172
Reflections with $I > 2\sigma(I)$	3513
Parameters	280
GOOF on F^2	1.097
R ($I > 2\sigma(I)$)	$R_1 = 0.0156$, $wR_2 = 0.0331$
R (all reflections)	$R_1 = 0.0172$, $wR_2 = 0.0341$
$\Delta\rho_{max}/\Delta\rho_{min}$, $e Å^{-3}$	1.041/–0.760

Table 2. Selected bond distances (Å) and bond angles (deg) for **I***

Bond	*d*, Å	Bond	*d*, Å
Pb(1)–O(2)^{i}	2.482(2)	Pb(2)–O(4)	2.601(2)
Pb(1)–N(1)	2.516(3)	Pb(2)–O(1)^{ii}	2.649(2)
Pb(1)–Cl(1)	2.8325(8)	Pb(2)–Cl(3)	2.8175(9)
Pb(1)–Cl(2)	2.8397(8)	Pb(2)–Cl(1)^{iii}	2.9138(8)
Pb(1)–Cl(3)^{v}	3.1749(8)	Pb(2)–Cl(2)	2.9735(8)
Pb(1)–O(1)^{i}	2.8199(21)	Pb(2)–Cl(2)^{vi}	3.1557(8)
Pb(2)–O(3)	2.444(2)		
Angle	ω, deg	Angle	ω, deg
O(2)^{i}Pb(1)N(1)	80.95(8)	O(1)^{ii}Pb(2)Cl(3)	162.21(5)
O(2)^{i}Pb(1)Cl(1)	85.01(6)	O(3)Pb(2)Cl(1)^{iii}	84.17(6)
N(1)Pb(1)Cl(1)	92.28(6)	O(4)Pb(2)Cl(1)^{iii}	135.25(6)
O(2)^{i}Pb(1)Cl(2)	84.07(6)	O(1)^{ii}Pb(2)Cl(1)^{iii}	82.01(5)
N(1)Pb(1)Cl(2)	83.31(6)	Cl(3)Pb(2)Cl(1)^{iii}	86.83(2)
Cl(1)Pb(1)Cl(2)	168.73(2)	O(3)Pb(2)Cl(2)	128.21(6)
O(3)Pb(2)O(4)	51.65(8)	O(4)Pb(2)Cl(2)	79.55(6)
O(3)Pb(2)O(1)^{ii}	83.94(8)	O(1)^{ii}Pb(2)Cl(2)	111.99(5)
O(4)Pb(2)O(1)^{ii}	86.07(8)	Cl(3)Pb(2)Cl(2)	85.02(2)
O(3)Pb(2)Cl(3)	81.17(6)	Cl(1)^{iii}Pb(2)Cl(2)	144.57(2)
O(4)Pb(2)Cl(3)	92.26(6)		

* Symmetry codes: ^{i} $1/2 - x, y + 1/2, 1/2 - z$; ^{ii} $x - 1/2, y + 1/2, z$; ^{iii} $-x, y + 1, 1/2 - z$; ^{iv} $-x, y - 1, 1/2 - z$; ^{v} $x, y - 1, z$; ^{vi} $-x, y, 0.5 - z$.

Table 3. Hydrogen bond lengths (Å) and bond angles (deg) for **I***

Contact D–H···A	Distance, Å			Angle D–H···A, deg
	D–H	H···A	D···A	
N(2)–H(2)···O(5)^{i}	0.86	1.96	2.781(5)	158
O(5)–H(5*B*)···O4^{ii}	0.86	1.98	2.807(6)	166

* Symmetry codes: ^{i} $x - 1/2, 1/2 - y, z - 1/2$; ^{ii} $1/2 - x, y + 1/2, 1/2 - z$.

RESULTS AND DISCUSSION

Complex **I** was hydrothermally obtained by the reaction of Pb^{2+} ion with H_2Bic ligand in weak acidic medium, in which the pH value of the reactants became one of the important factors for the crystalline form of **I**. In the IR spectrum of **I**, a broad band centered at 3482 cm^{-1} should be ascribed to the stretching vibrations of O–H, indicating the presence of water molecules in **I**. The absence of a characteristic band at ~1700 cm^{-1} indicates the deprotonation or proton shift of the carboxylic group in H_2Bic ligand. Correspondingly, the asymmetric (ν_{as}) and symmetric (ν_s) stretching bands for the carboxylate groups are observed at 1537, 1511, 1464, 1408, and 1377 cm^{-1}. Their slight difference may suggest the coexistence of the various binding modes of the carboxylate group in **I**. Thus, the IR spectrum of **I** is in good agreement with the single-crystal X-ray structural analyses.

Single crystal X-ray analysis reveals that complex **I** crystallizes in the monoclinic *C*2/*c* space group, exhibiting an infinite 2D layer with the helical Pb(II)-$HBic^-$ chains extended by bridging chloride anions. The asymmetric unit of **I** consists of two crystallographically independent Pb(II) atoms, three bridging chloride groups, two H_2Bic ligands with different protonation extent, and two lattice water molecules. As shown in Fig. 1, both unique Pb^{2+} ions are in the holodirected geometries with different coordination environments. Pb(1) is six-coordinated in an O_2NCl_3 donor set fulfilled by two bidentate chelating-bridging carboxylate O and one imidalzole N donors from two anionic $HBic^-$ ligands, and three separate chloride atoms. Instead, Pb(2) is seven-coordinated by four chloride anions and three carboxylate O donors from neutral H_2Bic and anionic $HBic^-$ ligands. The Pb–O, Pb–N, and Pb–Cl distances fall into the normal ranges (Table 2), which are comparable to those found in other reported Pb(II) complexes with aromatic polycarboxylate, triazolate, and/or chloride ligands [21–24].

Heterocyclic ligands exhibit deprotonation-dependent coordination modes in **I**. The neutral H_2Bic ligand with a proton shift from carboxylic group to imidazole ring presents its two carboxylate O donors to terminally coordinate with Pb(2) in a bidentate chelating mode and fulfill the metal coordination sphere of Pb(2). In contrast, the anionic $HBic^-$ ligand with the deprotonated carboxylate group serves as a bridging linker through carboxylate O and imidazole N donors to connect the adjacent Pb(1) ions to an infinite helical chain with the same chirality along the crystallographic *y* axis, which are further linked by Pb(2) ions and 3-fold homobridges (two μ_2-Cl^- and one μ_3-Cl^- bridges) to forming a 2D homochiral layer with the terminal H_2Bic ligands locating on the both sides (Fig. 2).

Furthermore, the adjacent 2D layers with the opposite helical chains are alternating arranged into a racemic 3D supramolecular framework through N–H···O and O–H···O hydrogen-bonding interactions between the imidazole moiety of the anionic $HBic^-$ ligand or the carboxylate group of neutral H_2Bic ligand and the lattice water molecule (Table 3 and Fig. 3).

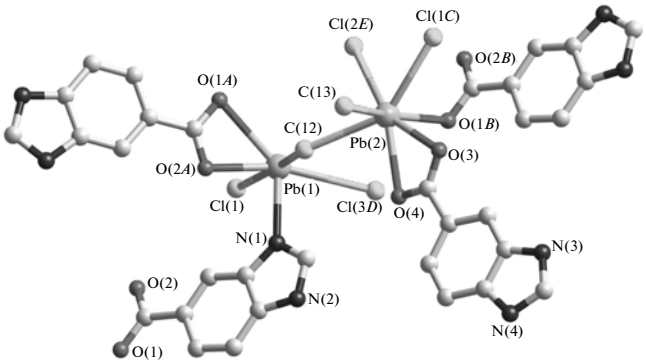

Fig. 1. Local coordination environments of Pb(II) atoms in **I** (H atoms were omitted for clarity, symmetry codes: (*A*) $1/2 - x, y + 1/2, 1/2 - z$; (*B*) $x - 1/2, y + 1/2, z$; (*C*) $-x, y + 1, 1/2 - z$; (*D*) $x, y - 1, z$; (*E*) $-x, y, 1/2 - z$).

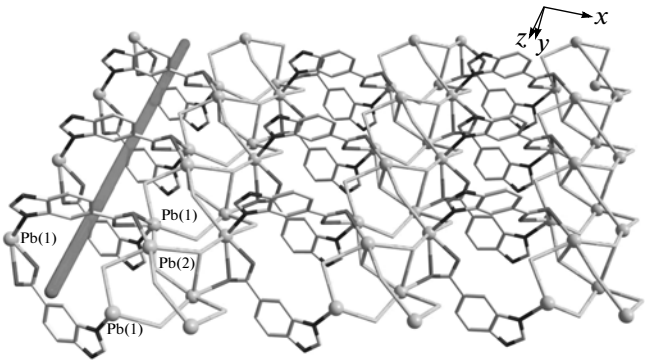

Fig. 2. 2D layer of **I** assembled from helical Pb(II)-$HBic^-$ chains and bridging chloride anions (Terminal coordinated H_2Bic ligands were omitted for clarity).

Thermogravimetric analysis experiment was carried out to further investigate the thermal stability of the title complex. As shown in Fig. 4, the first weight-loss process with an obvious endothermic peak at ~185°C appeared at 125°C and ended at 205°C, which should be ascribed to the loss of lattice water molecules (calcd: 4.1%, obsd: 4.0%). Then a short plateau was observed until a full decomposition at ~272°C occurred. And the obvious weight-loss beyond 272°C was due to the incomplete decomposition of the organic ligands in **I**.

Upon excitation at 400 nm, complex **I** in the solid state displays a strong emission at 565 nm (Fig 5). In contrast, the free H_2Bic ligand gives only one emission maximum at 550 nm [11]. Thus, the intense emission of **I** may be attributed to the intra-ligand charge transfer, which is much different from those originated from the ligand-to-metal charge transfer [13]. And the slight shift on the emission of **I** can be resulting from the slight energy-perturbation on the molecular orbits by the cation binding in different binding modes.

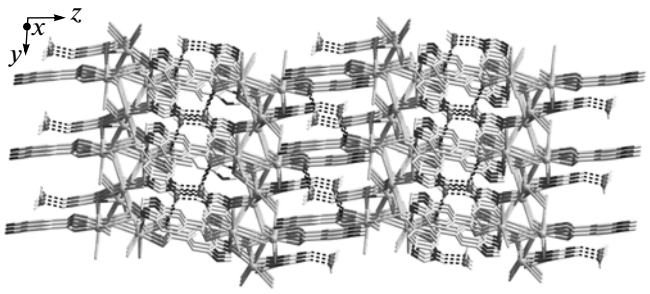

Fig. 3. 3D supramolecular framework of **I**.

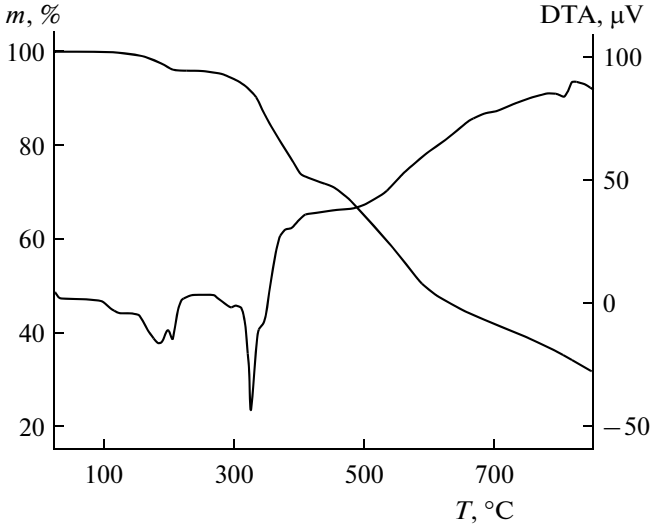

Fig. 4. TG–DTA curves for **I**.

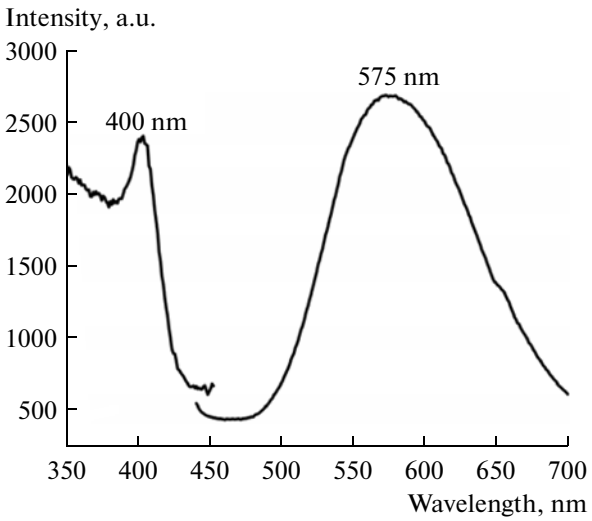

Fig. 5. Solid state excitation and emission spectra of **I** at room temperature.

ACKNOWLEDGMENTS

We gratefully acknowledged the financial supports from the National Natural Science Foundation of China (grants nos. 20871092, 20973125, 21171129, and 21173157), the Program for New Century Excellent Talents in University (NCET-08-0914), Tianjin Municipal Education Commission (2012ZD02), and the Natural Science Foundation of Tianjin (10JCZDJC21600).

REFERENCES

1. Chakrabarty, R., Mukherjee, P.S., and Stang, P.J., *Chem. Rev.*, 2011, vol. 111, p. 6810.
2. Forgan, R.S., Sauvage, J.-P., and Stoddart, J.F., *Chem. Rev.*, 2011, vol. 111, p. 5434.
3. Yang, E.-C., Liu, Z.-Y., Wu X.-Y., and Zhao, X.-J., *Chem. Commun.*, 2011, vol. 47, p. 8629.
4. Yam, V.W.W. and Lo, K.K.W., *Chem. Soc. Rev.*, 1999, vol. 28, p. 323.
5. Yoon, M., *Chem. Rev.*, 2012, vol. 112, p. 1196.
6. Kitagawa, J., Kitaura, R., and Noro, S., *Angew. Chem., Int. Ed.,* 2004, vol. 43, p. 2334.
7. Nowicka, B., Rams, M., Stadnicka, K., and Sieklucka, B., *Inorg. Chem.*, 2007, vol. 46, p. 8123.
8. Yang, E.-C., Liu, Z.-Y., Wang, X.-G., et al., *CrystEngComm*, 2008, vol. 10, p. 1140.
9. Yang, E.-C., Liu, Z.-Y., Shi, X.-J., et al., *Inorg. Chem.*, 2010, vol. 49, 7969.
10. Yang, E.-C., Liu, T.-Y., Wang, Q., and Zhao, X.-J., *Inorg. Chem. Commun.*, 2011, vol. 14, p. 285.
11. Guo, Z.-G., Yuan, D.-Q., Bi, W.-H., et al., *J. Mol. Struct.*, 2006, vol. 782, p. 106.
12. Liu, Z., Chen, Y., Liu, P., et al., *J. Solid State Chem.*, 2005, vol. 178, p. 2306.
13. Zhao, L.-N., Liu, T.-Y., Liu, Z.-Y., et al., *Z. Anorg. Allg. Chem.*, 2010, vol. 636, p. 2709.
14. Yao, Y.-L., Che, Y.-X., and Zheng, J.-M., *Inorg. Chem. Commun.*, 2008, vol. 11, p. 883.
15. Guo, Z.-G., Li, X.-J., Gao, S.-Y., et al., *J. Mol. Struct.*, 2007, vol. 846, p. 123.
16. Guo, Z.-G., Cao, R., Li, X.-J., et al., *Eur. J. Inorg. Chem.*, 2007, p. 742.
17. Parr, J., *Polyhedron*, 1997, vol. 16, p. 551.
18. *SAINT, Software Reference Manual, Madison* (WI, USA): Bruker AXS, 1998.
19. Sheldrick, G.M., *SADABS, Program for Empirical Absorption Correction of Area Detector Data*, Göttingen (Germany): Univ. of Göttingen, 1996.
20. Sheldrick, G.M., *SHELXTL, Structure Determination Software Programs*, Madison (WI, USA): Bruker Analytical X-Ray System, Inc., 2001.
21. Yang, E.-C., Li, J., Ding, B., et al., *CrystEngComm*, 2008, vol. 10, p. 158.
22. Durkin, J.J., Francis, M.D., Hitchcock, P.B., et al., *Dalton Trans.,* 1999, p. 4057.
23. Soudi, A.A., Morsali, A., and Moazzenchi, S., *Inorg. Chem. Commun.,* 2006, vol. 9, p. 1259.
24. Casas, J.S., Castellano, E.E., Ellena, J., et al., *Inorg. Chem.,* 2003, vol. 42, p. 2584.